PERGAMON

Deep-Sea Research II 50 (2003) 1611–1629

DEEP-SEA RESEARCH
PART II

www.elsevier.com/locate/dsr2

The recent seismo-volcanic activity at Deception Island volcano

Jesús M. Ibáñez*, Javier Almendros, Enrique Carmona, Carmen Martínez-Arévalo, Miguel Abril

Instituto Andaluz de Geofisica, Campus de Cartuja s/n, Universidad de Granada, 18071 Granada, Spain

Received 14 October 2002; received in revised form 10 December 2002; accepted 13 December 2002

Abstract

This paper reviews the recent seismic studies carried out at Deception Island, South Shetland Islands, Antarctica, which was monitored by the Argentinean and Spanish Antarctic Programs since 1986. Several types of seismic network have been deployed temporarily during each Antarctic summer. These networks have consisted of a variety of instruments, including radio-telemetered stations, autonomous digital seismic stations, broadband seismometers, and seismic arrays. We have identified two main types of seismic signals generated by the volcano, namely pure seismo-volcanic signals, such as volcanic tremor and long-period (LP) events, and volcano-tectonic (VT) earthquakes. Their temporal distributions are far from homogeneous. Volcanic tremors and LP events usually occur in seismic swarms lasting from a few hours to some days. The number of LP events in these swarms is highly variable, from a background level of less than 30/day to a peak activity of about 100 events/h. The occurrence of VT earthquakes is even more irregular. Most VT earthquakes at Deception Island have been recorded during two intense seismic crises, in 1992 and 1999, respectively. Some of these VT earthquakes were large enough to be felt by researchers working on the island. Analyses of both types of seismic events have allowed us to derive source locations, establish seismic source models, analyze seismic attenuation, calculate the energy and stress drop of the seismic sources, and relate the occurrence of seismicity to the volcanic activity. Pure seismo-volcanic signals are modelled as the consequence of hydrothermal interactions between a shallow aquifer and deeper hot materials, resulting in the resonance of fluid-filled fractures. VT earthquakes constitute the brittle response to changes in the distribution of stress in the volcanic edifice. The two VT seismic series are probably related to uplift episodes due to deep injections of magma that did not reach the surface. This evidence, however, indicates the high potential for future volcanic eruptions at Deception Island.

Contents

*Corresponding author. Tel.: +34-958-248910; fax: +34-958-160907.
E-mail address: ibanez@iag.ugr.es (J.M. Ibáñez).

0967-0645/03/$ - see front matter
doi:10.1016/S0967-0645(03)00082-1

1. Introduction

Deception Island is a volcanic island located at 62°59′S and 60°41′W in the South Shetland Islands region (Fig. 1). It constitutes a back-arc stratovolcano with a basal diameter of ~30 km. The volcano rises ~1400 m from the seafloor to a maximum height of 540 m above sea level. The 15-km-diameter island is horseshoe-shaped and displays a flooded caldera (Port Foster) with dimensions of about 6 × 10 km and maximum depth of 190 m. The caldera wall is breached by a 500-m-wide passage named Neptune's Bellows. Glaciers cover almost half of the island, mainly on Mount Pond and Mount Kirkwood in the east and south, respectively.

The geodynamic setting of the Deception Island region is characterized by interactions among small tectonic units. The Drake microplate (Fig. 1) represents the remnants of a subduction that once extended beneath the western margin of the Antarctic Peninsula. This subduction process finished progressively from southwest to northeast, but a slow subduction activity at the South Shetland Trench, northwest of the South Shetland Islands, still continues (e.g., Barker, 1982; Pelayo and Wiens, 1989; Kim et al., 1995; Lawver et al., 1995; Robertson et al., 2001).

The Bransfield Strait is a consequence of the rifting and separation between the South Shetland microplate and the Antarctic Peninsula. There are three active extensional basins that show evidence of volcanism and normal faulting. The axis of the central basin is marked by a series of seamounts between Deception and Bridgeman Islands, many of which have recently been active (Gracia et al., 1996; Lawver et al., 1996; Gracia et al., 1997). However, the crustal thickness of 12–30 km is consistent with extrusion through rifted continental crust rather than seafloor spreading (Bialas et al., 1990; Grad et al., 1992; Barker and Austin, 1994; Grad et al., 1997; Janik, 1997; Barker and Austin, 1998; Prieto et al., 1998; Barker et al., 2001). Based on the seismicity and volcano spatial distribution, Barker and Austin (1998) have suggested south-westward propagation of the Bransfield Rift. The NW-SE extension of ~10 mm/yr has been attributed to rollback of the subducted slab (Barker and Austin, 1998; Dietrich et al., 2001).

The seismicity in Bransfield Strait has characteristics of rift extension, subduction, and volcanism. Virtually all earthquakes in the region are either shallow (<40 km depth) and consistent with rifting, or deep and consistent with subduction of the Drake plate (Pelayo and Wiens, 1989; Ibáñez et al., 1997). Many of the shallow earthquakes tend to cluster near volcanoes, indicating a likely volcanic or volcano-tectonic origin (Pelayo and Wiens, 1989; Robertson et al., 2001). Seismic activity is specially pronounced at Deception Island volcano (Pelayo and Wiens, 1989; Lee et al., 1998; Robertson et al., 2001).

Most rocks on Deception Island have been classified relative to the undated caldera-forming eruption (Martí and Baraldo, 1990). All exposed

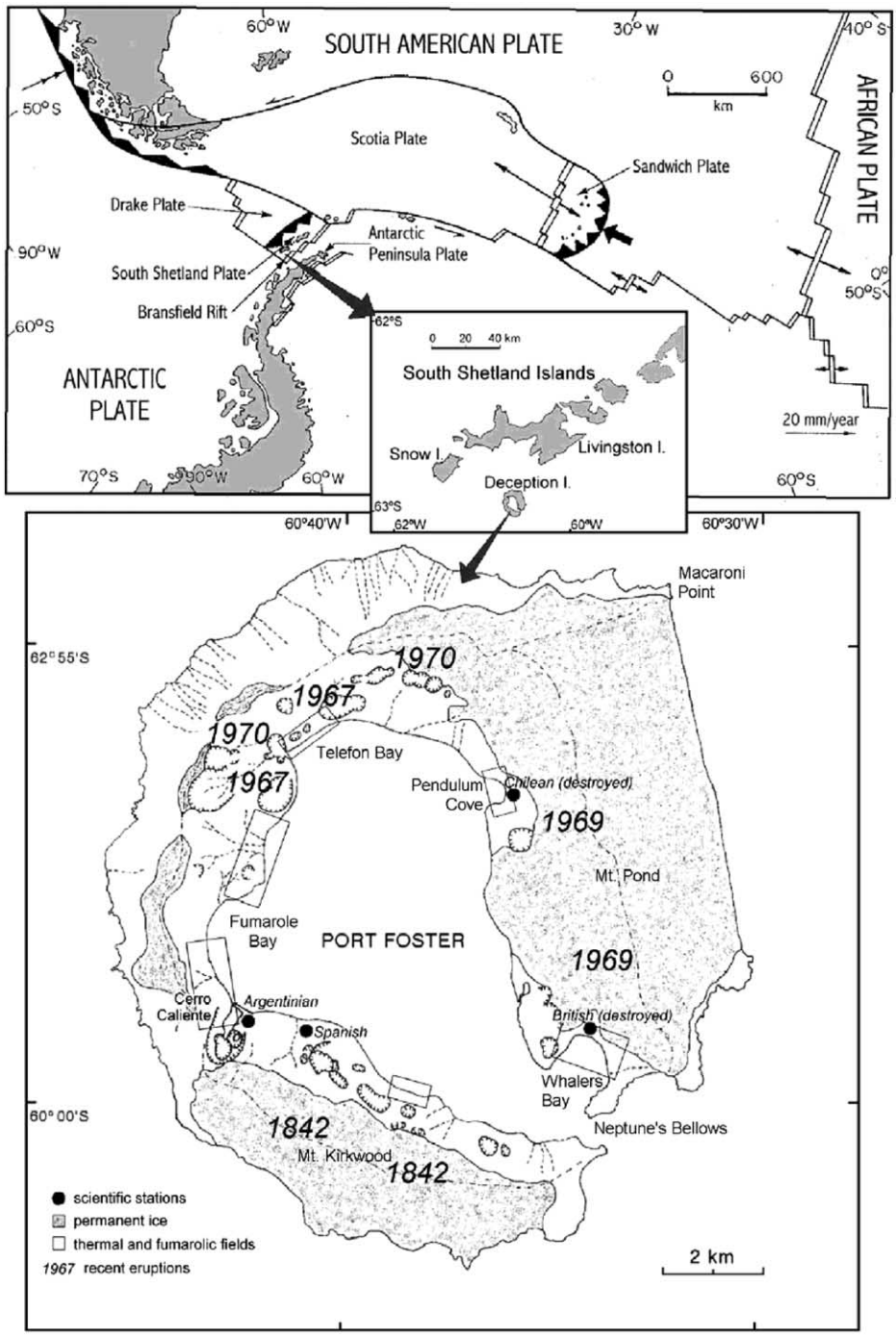

Fig. 1. Location of Deception Island in the South Shetland Islands region and map of Deception Island showing the main volcanological features.

rocks have normal magnetic polarity, indicating that they are younger than 700 ka; the oldest dated age of the pre-caldera deposits is 200 ka (Keller et al., 1991). The standard sequence has been developed by Birkemajer (1992), and correlated with shallow-penetration seismic reflection sections in Port Foster by Rey et al. (1997). The pre-caldera rocks are exposed on sea cliffs and parts of the caldera wall, and are composed of tuffs and agglomerates with interspersed lava flows and scoria horizons. The post-caldera deposits include basaltic lavas and scoria at higher elevations and pyroclastic cones around Port Foster where the magma interacted with seawater. It is generally accepted that the post-caldera deposits have been controlled by the ring-fracture system, with most eruptions occurring near the margins of the caldera (Baker et al., 1969; Smellie, 1990).

The caldera at Deception Island volcano has been traditionally described as a classic example of collapse caldera that formed about a ring fracture following one or more voluminous eruptions of andesitic magma (Baker et al., 1975; Smellie, 1988). However, there are other models of caldera formation, for example the incremental growth in response to a series of moderate-sized eruptions (e.g., Walker, 1984). On the basis of the structural data and other lines of evidence, Rey et al. (1995) and Martí et al. (1996) argue that the Deception Island caldera is a tectonic depression that was formed progressively by passive normal faulting along sets of nearly orthogonal normal faults that cut across the island and follow the regional trends. Structural mapping and shallow-penetration seismic reflection studies within Port Foster show that the architecture of Deception Island is controlled by three major fault systems (Rey et al., 1997). The first one is a NE–SW striking system that is consistent with the regional extensional regime of Bransfield Strait and controlled the vent alignment during the 1967 and 1970 eruptions. Several faults in this system cut across the caldera. A second system strikes at $\sim 120^{\circ}$N, defines the caldera wall near Mount Kirkwood in the south, and parallels an axis of submarine volcanic cones in the southern part of Port Foster. A third system strikes at $\sim 170^{\circ}$N, and includes the Macaroni fault that forms an 8 km length of the island's NE coastline. In support of this model, Rey et al. (1995) and Martí et al. (1996) note the absence of circular sections of the postulated ring fault and radial dikes and fractures within the caldera. They infer that nearly all the post-caldera eruptions have been located on linear faults, some of which lie outside the hypothetical ring fault, while others cut the caldera. One implication of their model is that the caldera may be underlain by much less extensive and perhaps discontinuous magma reservoirs whose position is controlled by the location of faults.

Deception Island is the most active volcano of the South Shetland Islands region, having erupted at least 6 times since it was first visited 160 years ago. All historical eruptions have been relatively small in volume. They have occurred at locations near the coast of the inner bay, all around the caldera (Fig. 1). Some of the eruptive episodes have included simultaneous eruptions of chemically distinct lavas from multiple vents (Newhall and Dzurisin, 1988). The first report of an eruption at Deception Island dates back to 1842, when a "wall of fire" was observed by whaling ships, related to a set of craters that formed below Mt. Kirkwood in the southwest part of the island (Roobol, 1973). From ice records at surrounding islands, explosive eruptions are inferred to have occurred in 1912 and 1917 (Orheim, 1972). The ice record in James Ross Island, 200 km from Deception (Aristarain and Delmas, 1998), suggests that an important eruption occurred in the 19th century. This eruption may have been the largest one on the island in the last 350 years. Three eruptions between 1967 and 1970 were observed directly and are well documented. In December 1967, two vents developed simultaneously at sites located ~ 2 km apart. One of them was a submarine eruption that gave birth to a new island in Telefon Bay, while the other occurred inland, between Telefon Bay and Pendulum Cove. A second eruption occurred in February 1969, when fissures opened in the ice on the west-facing slopes of Mt. Pond, accompanied by pyroclastic emissions. The last eruption took place in August 1970, when additional activity along the northern edge of Telefon Bay formed a chain of new craters and modified the coast line.

The chemical differences observed between the lavas suggest that the eruptions were fed by small isolated magma reservoirs (Roobol, 1979). Likewise, the synchronicity of some historical eruptions and the fact that they occurred throughout the caldera are most easily explained if the volcanic activity resulted from small magma bodies that rose up from a large magma chamber extended across the whole caldera. Leaks of silicic magma along ring fractures have preceded some large caldera-forming eruptions (e.g., Bacon, 1985), and one could speculate that the recent activity at Deception Island may be a long-term precursor of a larger eruption. The most accepted interpretation, however, assumes that Deception Island is presently in an early stage of the infilling of the caldera by small-volume eruptions (Roobol, 1982).

Evidences for present-day volcanic activity at Deception Island include fumaroles and hydrothermal activity (Fig. 1), resurgence of the floor of Port Foster, and seismicity. Fumaroles and hot springs with temperatures up to 110°C encircle Port Foster, while hydrothermal vents have been reported outside the island (Smellie, 1990). The analysis of repeated bathymetric surveys of Port Foster obtained between 1949 and 1993 allowed Cooper et al. (1998) to identify three regions that are shallowing at rates of up to 0.5 m/yr. High rates of shallowing in near-shore regions to the north of Fumarole Bay and in Telefon Bay could be entirely due to sedimentation, but a region of rapid shallowing in NE Port Foster is attributed to volcanic resurgence. Uplift has continued more recently in this area, with 5 m measured between 1990 and 1999. This region lies within an EW-trending belt of earthquake epicenters across Port Foster (Vila et al., 1992; Ibáñez et al., 2003), displays high seismic attenuation in the shallowmost crust (Vila et al., 1995), and is site of magnetic and gravity anomalies (Ortiz et al., 1992).

2. Seismicity of Deception Island

Based on the experience from the successive field surveys carried out at Deception Island volcano, the local seismicity has been classified in two main groups: volcano-tectonic (VT) earthquakes and long-period (LP) seismicity (which includes LP events and volcanic tremor). A third group of seismo-volcanic events are named hybrids, since they share characteristics from both of the main groups.

VT earthquakes are local earthquakes generated within the volcanic edifice. At Deception Island, for example, they usually display $S-P$ times smaller than 3–4 s. VT earthquakes are dominated by a double-couple mechanism, and often characterized by impulsive P-wave onsets and clear S arrivals. The spectral content is broad, with significant energy up to 30 Hz. In Fig. 2 we plot three examples of different types of tectonic earthquakes recorded at Deception Island. Note the clear differences in the temporal and spectral signatures. The hypocenters of VT earthquakes are not homogeneously distributed at Deception Island. For example, Vila et al. (1992, 1995) provided a map of the seismicity for the 1986–1991 period showing epicenters located all over the island; Ibáñez et al. (2000) located earthquakes recorded during the period 1994–1998 along a NE–SW fracture system near the Spanish base; and finally Ibáñez et al. (2003) located the epicenters of VT earthquakes belonging to the 1999 series, which were confined mostly to Port Foster. VT earthquakes at Deception Island are usually shallow, low-magnitude events. However, some earthquakes with magnitude greater than 3.5 have been recorded, and there is evidence of the occurrence of larger earthquakes near Deception Island, with magnitudes greater than 5.0 (Pelayo and Wiens, 1989). The source of the VT earthquakes is associated to the brittle failure of parts of the volcanic edifice in response to changes in the distribution of local or regional stresses. Stresses may change for example due to interactions of water with hot materials (Vila et al., 1995; Correig et al., 1997) or to the effects of shallow magma injections (Ortiz et al., 1997; Ibáñez et al., 2003).

LP seismicity is characterized by a quasi-monochromatic spectral content. The most frequent type of LP seismicity at Deception Island are the LP events, which constitute signals with a spindle-shaped envelope and durations smaller

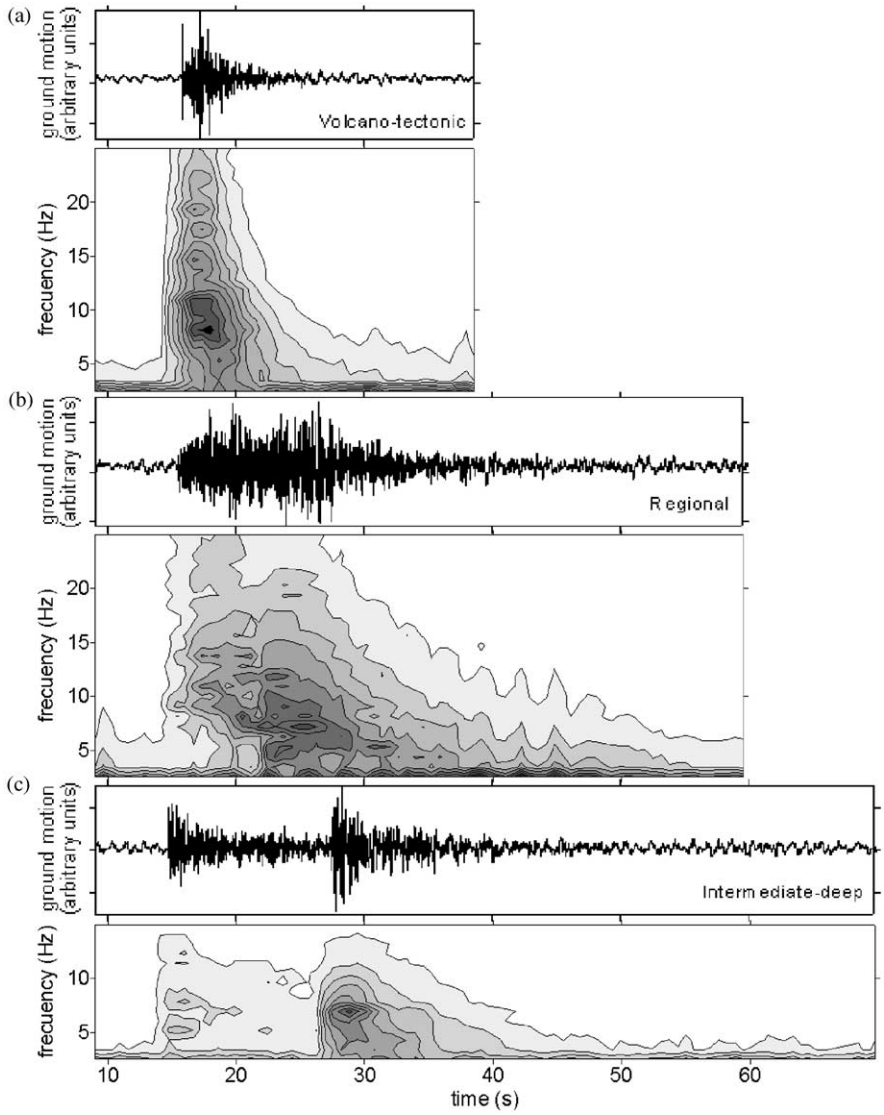

Fig. 2. Example of vertical-component velocity seismograms and array-averaged spectrograms for (a) a VT earthquake; (b) a regional earthquake; and (c) an intermediate-deep earthquake. All these signals have been recorded at Deception Island volcano. Spectrograms are obtained by dividing the seismograms into overlapping 2.56-s windows and averaging over the whole seismic array.

than 60 s. In some cases, a high-frequency phase precedes these events. In Fig. 3 we show examples of three types of LP events with different spectral content and duration. The location of the source of these pure volcanic signals has been derived from seismic antenna analyses (Almendros et al., 1997, 1999). Alguacil et al. (1999) and Ibáñez et al. (2000) have identified two different types of spectral behavior in the low-frequency band of these signals. The most common corresponds to a series of non-regularly spaced peaks, while the second shows regularly spaced harmonics of a fundamental peak. In the first group two subsets are differentiated by the frequency of the main

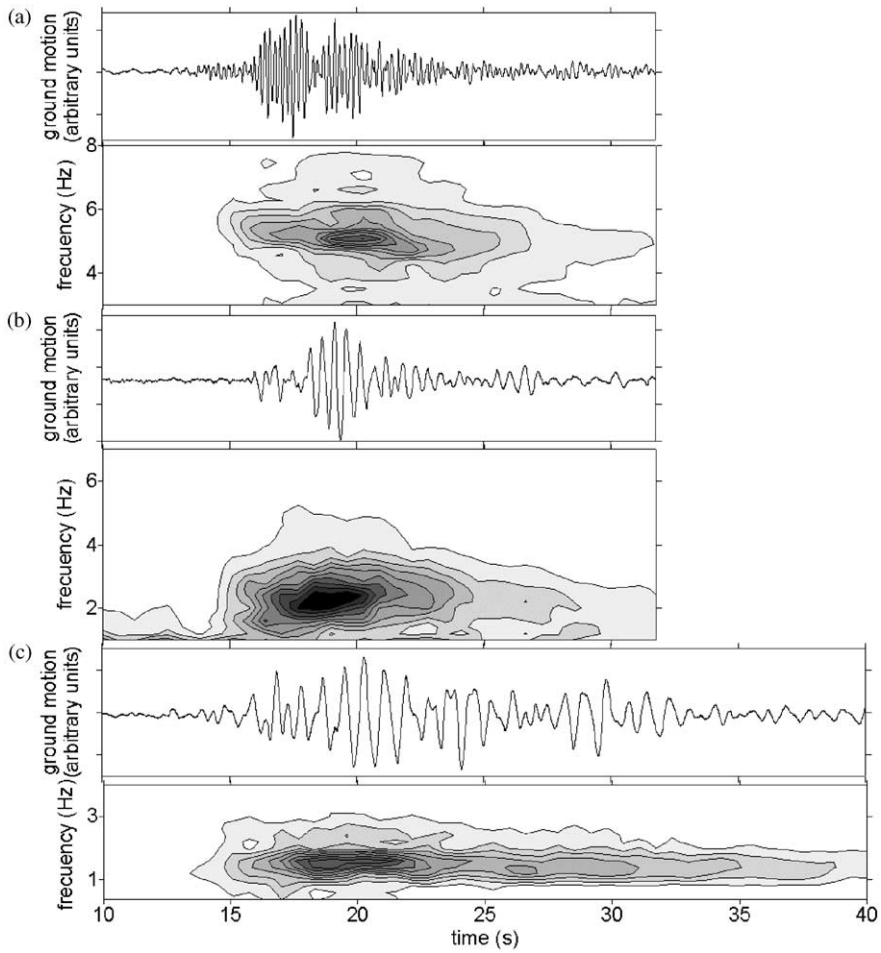

Fig. 3. Example of vertical-component velocity seismograms and array-averaged spectrograms for LP events recorded at Deception Island, with frequency contents centered at (a) 5 Hz; (b) 2.5 Hz; and (c) 1.5 Hz.

peak. The source processes that generate the LP seismicity involve a volumetric component due to the resonance of fluid-filled cavities (Chouet, 1996).

Volcanic tremor is a monochromatic signal with duration longer than that observed for LP events. Episodes of tremor that last from minutes to several hours and days have been observed at Deception Island volcano. In Fig. 4 we show a 3-h sample of volcanic tremor. Models of tremor generation are based on degassing, fluctuations of the gas, resonance of conduits, etc (e.g. Chouet, 1992; Julian, 1994). Those models considering the resonance of open conduits have been complicated by introducing different geometries of the resonance system. Although they are enough to explain some tremor signals, in other cases the geometrical considerations need to be completed by including in the tremor models data about the reology of the fluids and their dynamics (Chouet, 1996). Some results, which integrate observations of tremor and LP, show evidences that both type of events share similar source regions and processes (Almendros et al., 1997, 2001). Tremor and LP events are supposed to be different manifestations of the same process. An LP event is the

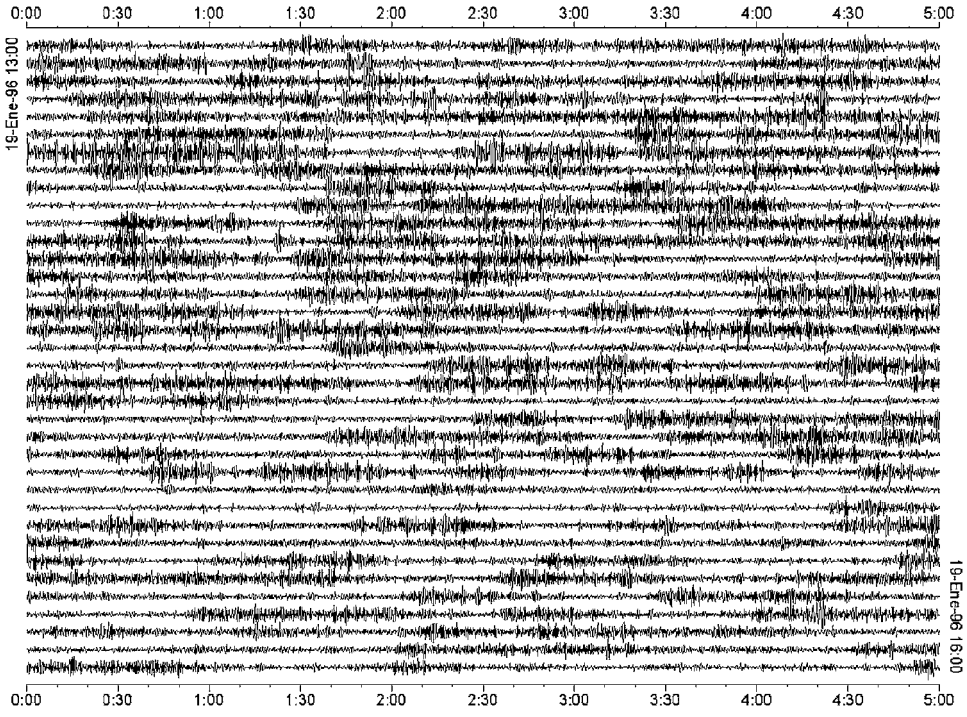

Fig. 4. Example of vertical-component velocity seismogram corresponding to continuous recording of 3 h of volcanic tremor at Deception Island volcano.

response to a sudden pressure transient within a fluid-filled crack, while tremor is the response to continuous fluctuations of pressure.

Hybrid events are signals that contain both double-couple and volumetric components. They are characterized by an initial high-frequency phase similar to a VT earthquake, followed by a monochromatic signal similar to those shown by the LP events (Fig. 5). In some cases, LP events with an energetic initial high-frequency onset could be confused with hybrids. While the low-frequency signature is originated in both cases by the resonance of a fluid-filled cavity, in the case of hybrid events the initial pressure step that triggers the resonance is caused by a brittle failure process. Recently, Ibáñez et al. (2003) have distinguished in Deception Island signals that might be interpreted as hybrids. They have found a few VT earthquakes that are closely followed by LP events. Both parts of the signals share a similar source region. This region coincides with an area of VT earthquake generation, which constitutes our only clue as to the hybrid character of the signals. In reality, only a detailed analysis of the source mechanisms using a network with appropriate coverage could settle the question of whether these signals are LP events or hybrids.

3. Review of recent seismic studies

3.1. History of seismic monitoring at Deception Island

The seismic monitoring of Deception Island volcano began in the 1950s when a seismometer was deployed at the Argentinean base. Data from this station were recorded continuously on smoked paper drum until the end of the 1960s when the series of eruptions that took place in the island forced the evacuation of the bases. Seismic records obtained during this period show the frequent

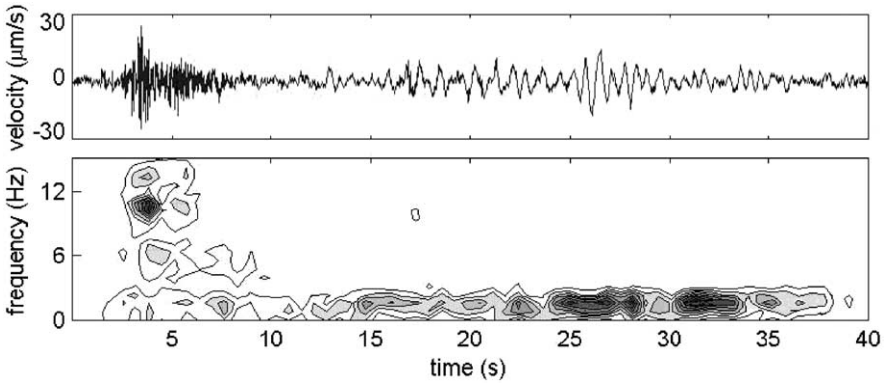

Fig. 5. Example of vertical-component velocity seismogram and array-averaged spectrogram for a signal interpreted as a hybrid event (Ibáñez et al., 2003).

occurrence of local seismicity, including VT earthquakes, LP events, and episodes of volcanic tremor. The rate of occurrence of seismic events increased just before each of the 1967–1970 eruptions, which emphasizes the usefulness of seismic monitoring as a forecasting tool at Deception Island. Regional and teleseismic earthquakes also were detected, but due to the lack of adequate coverage only earthquakes with magnitude 5 or above could be located.

From 1970 to 1986 there are no seismic records from Deception Island. In 1986 the monitoring of the seismic activity was re-established through summer field surveys carried out by Argentinean and Spanish researchers, with the result of a temporary control of the seismic activity of the volcano (Fig. 6). Several types of seismic deployments have been used (Fig. 3). Between 1986 and 1988 a vertical short-period seismic station recording on a thermal paper drum was used, at a location near the Argentinean base. Between 1989 and 1991, seismic data were recorded by a network composed of five short-period seismic stations with radio telemetry. In this period, several VT earthquakes and a few volcanic tremor episodes were recorded. Vila et al. (1992, 1995) and Correig et al. (1997) studied this seismic activity and provided the first epicentral map of the VT activity of Deception Island volcano. These authors also proposed a model of the occurrence of the activity based on the degasification of an aquifer in contact with deep hot materials. In average, the energy of the tectonic and volcanic quakes recorded between 1986 and 1991 was quite low.

This situation changed in January 1992, when an important increase in the number and magnitude of the seismic events was detected (Ortiz et al., 1997). More than 750 VT earthquakes were recorded in less than 2 months. Some of these earthquakes and even a few episodes of volcanic tremor were felt. During this survey the only available seismic instrument was a three-component short-period seismometer deployed near the Argentinean base. Although the epicentral area of the recorded activity could not be determined accurately, indirect evidence shows that the source area was probably located under Port Foster, just 2–3 km from the shoreline. Observations of small gravity irregularities and magnetic anomalies correlated with the successive seismic swarms suggest that a magmatic injection took place during this increase of seismic activity (Ortiz et al., 1992, 1997; García et al., 1997). However, it had not enough energy to reach the surface. Changes in fumarolic emissions and a possible deformation process near the Argentinean base support the hypothesis of magmatic injection. The seismic and gravimetric evidences of this activity started to decline in February 1992.

During the 1992–1993 and 1993–1994 field surveys new seismic stations were deployed near

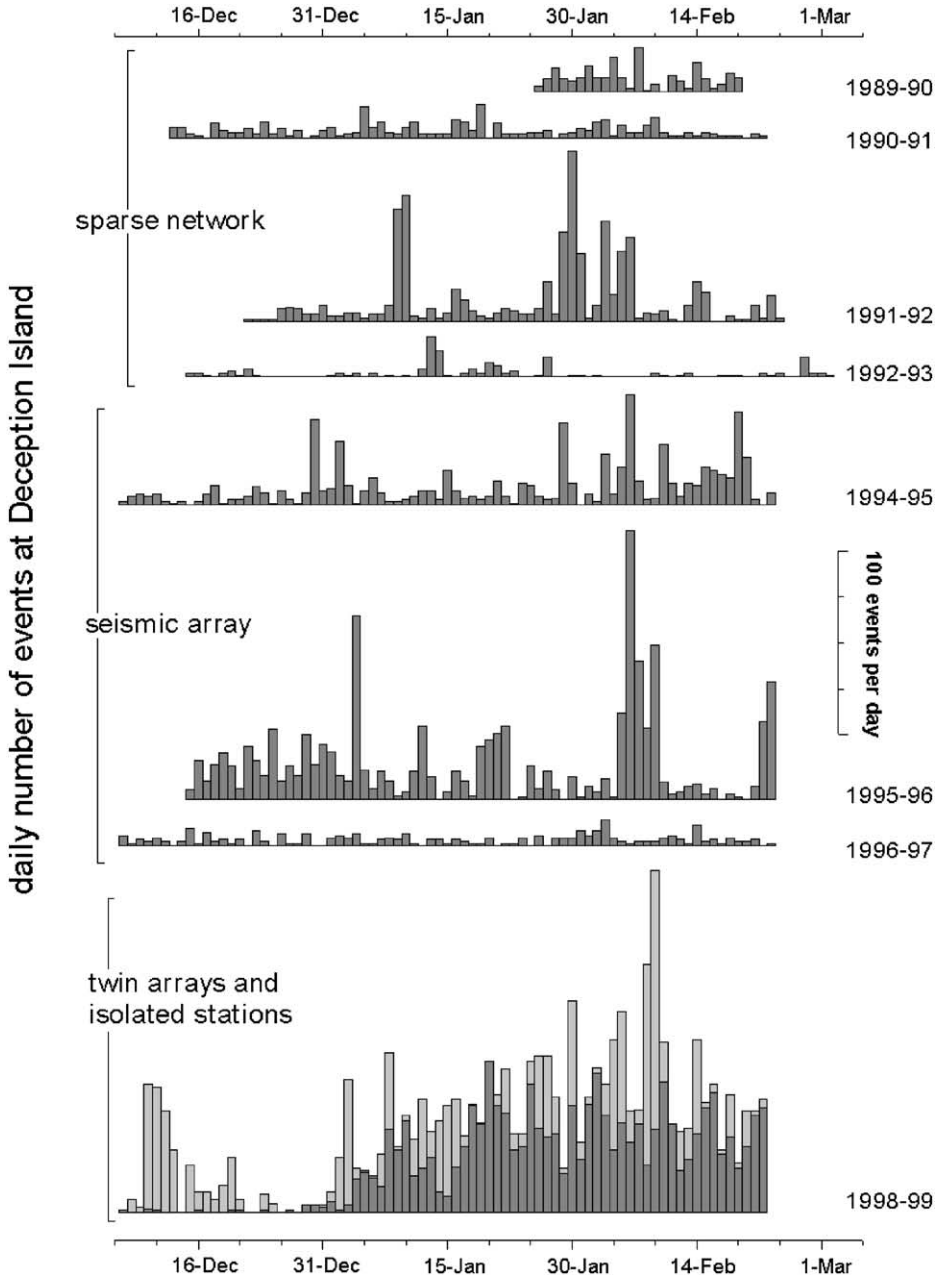

Fig. 6. Histogram of the daily number of seismo-volcanic earthquakes recorded at Deception Island during the summer field surveys in the period 1989–1999, with the exception of the 1997–1998 survey. In the 1998–1999 survey we show separately the VT earthquakes (dark gray) and LP events (light gray).

the Argentinean and Spanish bases to study the continuity of the seismic swarm of January 1992, although the activity had decreased to the pre-1992 level (Fig. 6). However, a change in the characteristics of the seismic activity was observed. Starting on December 1992, the number of VT

earthquakes clearly decreased, while the number of LP events and tremor increased (Felpeto et al., 1994). Since the seismic stations deployed on the island were powerless to locate or analyze the LP seismicity, the objectives of the seismic experiments were modified and the use of seismic antennas was introduced.

3.2. Seismic antenna surveys

The increasing contribution of LP events and tremor to the overall seismicity of Deception Island volcano motivated the introduction of seismic antennas. Seismic antennas allow complete analyses of the seismic wavefield and are able to provide useful information about the nature of LP events and volcanic tremors. In 1994, a small-aperture seismic antenna was set up near the Spanish Base "Gabriel de Castilla" to track the seismo-volcanic sources. This antenna was deployed again for the summer field surveys between 1995 and 1997. Preliminary reports obtained from analyses of the array data (Alguacil et al., 1999) confirmed the existence of VT earthquakes, LP events, and sustained tremors near the array site, in an area south of Cerro Caliente (see Fig. 1). Ibáñez et al. (1997) reported the presence of intermediate depth (30–120 km) and shallow earthquakes (0–30 km) in the area. Almendros et al. (1997) showed that some volcanic tremor episodes were generated by the multiple occurrence of low-energy LP events. Almendros et al. (1999) introduced a modification of the zero-lag cross-correlation technique taking into account the circular geometry of the incoming wave fronts. Using this technique, the epicentral locations of a subset of LP events were estimated to be close to the antenna, at distances of a few hundred meters southwest of the array site.

In 1998, two semi-circular seismic antennas were deployed along the inner coast of the western side of Deception Island (Fig. 7), at a distance of about 2 km. The objective of the two-antenna deployment was the investigation of the shallow velocity structures under the arrays and the use of a joint location method to improve the location capabilities of the antennas. The presence of the seismic antennas has allowed for the analysis of the LP seismicity generated in different regions of the island. Moreover, the source locations of several hundreds of VT earthquakes recorded in January and February 1999 were estimated using an inverse ray-tracing procedure (Ibáñez et al., 2003).

3.3. Seismic attenuation studies

Martínez-Arévalo et al. (2003) studied the seismic attenuation in the short-distance and high-frequency range using *P*, *S*, and coda waves. They applied different techniques, including both frequency-dependent and frequency-independent methods such as broadening of the pulse for direct *P*- and *S*-waves, coda normalization for *S*-waves, single back-scattering for coda waves, and the spectral method. The results show that Q values are significantly smaller, for the entire frequency range analyzed (6–30 Hz), than those found in other volcanic and tectonic areas. The attenuation for *P*-waves is greater than for *S*-waves in the frequency-independent methods, with a Q_β/Q_P ratio that ranges between 1.9 and 3.2. Q factors obtained for *S*-waves show clear differences depending on the method used. The coda normalization method has supplied significantly higher Q values (Q_d) than the other two methods (Q_β). This discrepancy is due to the fact that coda normalization and single back-scattering methods eliminate the contribution of the near-surface attenuation. Comparing Q_β and Q_d, the near-surface attenuation under the recording site, Q_κ, was estimated. Q_d displays an anomalous frequency dependence, with a minimum value at 21 Hz. This pattern was interpreted as the effect of strong scattering of the seismic waves in the source area. Q_c values clearly depend upon frequency and lapse time. The lapse time dependence could be interpreted as a depth dependence of the seismic attenuation in Deception Island volcano. Separating the contribution of intrinsic and scattering attenuation, Martínez-Arévalo et al. (2003) found that the scattering attenuation is predominant over the intrinsic effects. All these observations suggest a highly heterogeneous structure for Deception

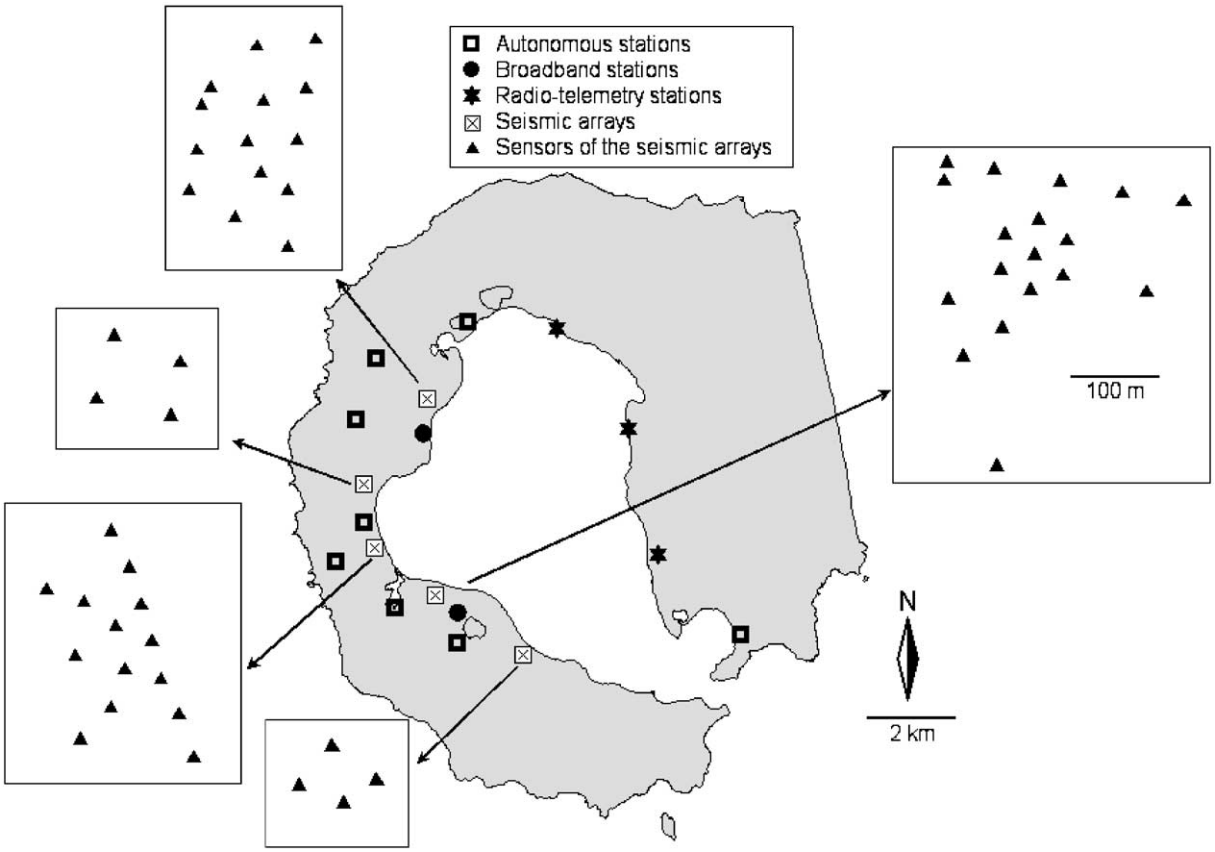

Fig. 7. Map of Deception Island volcano showing the position of the seismic stations and antennas deployed during the different seismic experiments carried out since 1994.

Island volcano. Similar observations were done by Havskov et al. (2003) using different techniques.

4. The 1999 seismic crisis

The seismic crisis that occurred in January–February 1999 represents a good example of the intense seismic swarms that occasionally shake Deception Island volcano. During the month of December 1998 only a few events were recorded (8 VT earthquakes), a rate similar to that reported by Ibáñez et al. (2000) for previous years. However, this trend was suddenly modified on January 1, 1999, when the number of local earthquakes suddenly increased (Fig. 8). The seismic swarm reached its maximum daily number of events on January 20, with the occurrence of 80 VT earthquakes. When the field survey finished, the seismic activity was still high, more than 50 earthquakes/day. At the bottom of Fig. 8 we show a histogram of the local earthquakes recorded by a seismic station deployed at the Spanish Base, which continued its operations for up to 2 months after the main field survey ended. We can infer from this figure that, although in March the activity was decreasing, at the end of this month there was a new increase. During the summer period more than 3000 earthquakes were detected and 863 have been analyzed. Several earthquakes had magnitude-momentum greater than 2.5. At least two of them were felt by the staff working on the island,

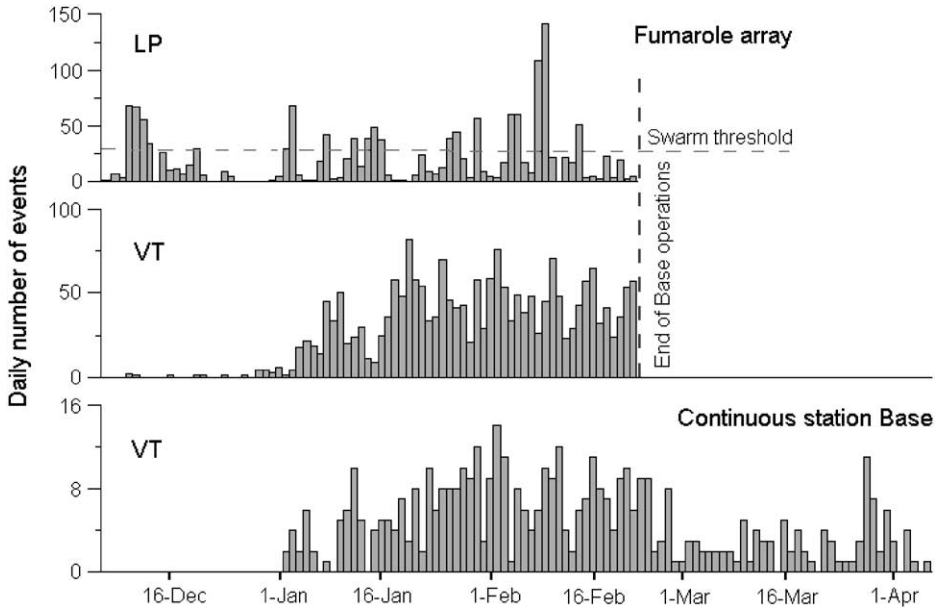

Fig. 8. Histograms of the daily number of LP events (top) and VT earthquakes (middle) detected during the 1999 crisis by the Fumarole seismic antenna, and VT earthquakes recorded by the continuous station at the Spanish Base between December 1998 and April 1999 (bottom).

one of them at the beginning of the series, on January 11, and the second in January 20, with magnitudes of 2.9 and 3.4, respectively. Both events represent a qualitative change in the seismic pattern, because since the 1991–1992 crisis no earthquakes of this magnitude had been reported (Ortiz et al., 1997). LP seismicity appeared in swarms that lasted a few days and alternated with rest periods of several days. A total of 1800 LP events were recorded, with peak activity reaching about 150 events/day. Using a lower limit of 30 events/day to define an LP swarm (Ibáñez et al., 2000), there were nine swarms distributed randomly throughout the recording period (Fig. 8). This pattern coincides with that previously observed for the LP seismicity (see Fig. 6), and therefore the LP activity in 1998–1999 was considered normal for the area.

Hypocenters of the VT earthquakes and hybrids were determined using the apparent slowness, back-azimuth, and $S-P$ time to perform an inverse ray-tracing source location (Ibáñez et al., 2003). The $S-P$ time fixes the distance to the source; the back-azimuth is the direction to the epicenter; and the apparent slowness provides the incidence angle. The hypocentral distribution (Fig. 9) indicates that the seismicity is clustered at a focal depth of $\sim$2 km near the Fumarole array and mostly toward the northeast. More than 90% of the events are clustered in a volume of around 10 km^3. However, deeper and more distant events also were found, with focal depths reaching 10 km and epicentral distances up to 18 km. The main cluster has two denser regions (see the dashed lines in Fig. 9). The first one extends about 3 km in a direction of about 45°N, with focal depths between 1 and 4 km. The second is longer but more diffuse, and extends toward 80°N. Most part of the seismicity is located within the inner bay of Deception Island and apparently dips at an angle of about 45°. Hybrid event locations coincide with the cloud of VT earthquakes. Most of them are contained in the branch of seismicity extending toward 80°N.

The VT earthquakes analyzed span a magnitude range from −0.8 to 3.4. These magnitudes allow us to track the energetic evolution of the seismic series, as well as estimate the cumulative seismic

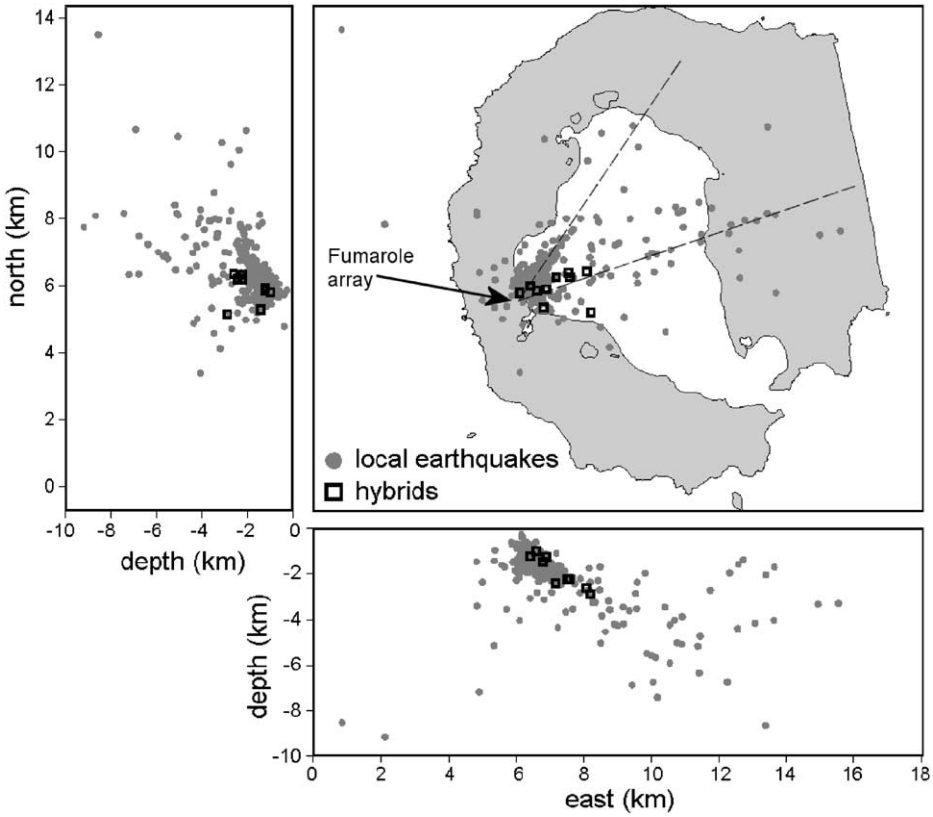

Fig. 9. Hypocentral locations of the VT earthquakes (dots) and hybrid events (squares) recorded by the Fumarole Bay seismic antenna during the 1999 crisis (from Ibáñez et al., 2003). The dashed lines represent the alignment of epicenters along preferred directions.

moment. Except for the two larger earthquakes mentioned above, the energy release is more or less steady in time. The distribution of magnitudes is nearly the same throughout the series. The stress drop of the VT earthquakes, derived from the magnitude analysis, is very low. More than 95% of the stress drop values are concentrated between 0.1 and 4 bar. Corner frequencies range from 40 Hz for the smallest events to 6 Hz for the largest ones (these values do not include those events that saturated the records). Using Brune's model (Brune, 1970) we found that the source dimensions range from 10 m up to 200 m, with an average of 50 m. Using Madariaga's model (Madariaga, 1977) the dimensions obtained are smaller, and range from 5 to 120 m, with an average of 30 m. In any case, the estimates of the source dimensions indicate clearly the small size of the fractures involved in the generation of earthquakes during the seismic series. These tiny fractures are primarily concentrated in a small focal volume, inside of which we have detected hundreds of events.

5. Source models

In this section, we will describe the models generally assumed to explain the origin of the LP seismicity and the generation of VT earthquakes at Deception Island. We also will explain the reason for their occurrence in swarm-type sequences.

5.1. Model for pure volcanic signals

The conceptual model proposed by Ibáñez et al. (2000) to explain the origin of the pure volcanic

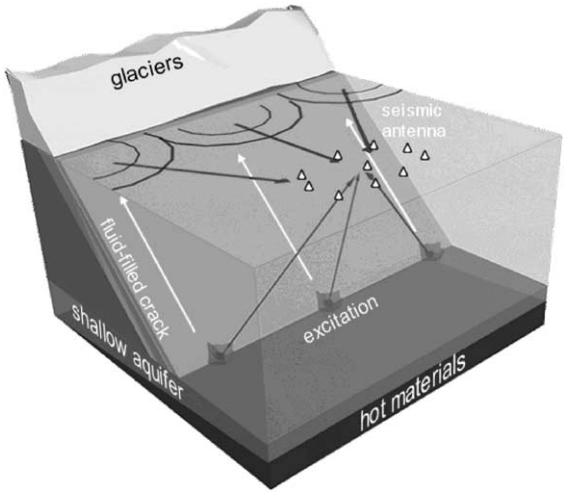

Fig. 10. Sketch of the seismic source model proposed by Ibáñez et al. (2000) to explain the origin of the LP seismicity at Deception Island volcano (see text for explanations).

signals (Fig. 10) can be summarized as follows: a sudden pressure step occurring at depth in a fluid-filled crack puts the crack itself in auto-oscillation. This pressure step may be caused for example by a sudden phase change of the hydrothermal fluids. A two- or three-dimensional source model is necessary to explain the spectral characteristics of the acoustic resonance. The high-frequency waves are produced by the phase change occurring at some position along the lower edge of the crack. The low-frequency waves are generated by the resonance of the whole crack and therefore propagate with similar back-azimuths, depending on the spatial orientation of the crack. The complex low-frequency wave pattern is due to the mixed contribution of P, SV, and SH waves radiated by the source (according to the model developed by Chouet, 1986, 1988, 1992) and to the generation of surface waves in the multiple-layered structure of the island, composed of frozen soil and different volcanic layers. This model could provide a unique source mechanism for LP events and volcanic tremors. The different spectra can be associated with different crack dimensions and properties. Assuming the model developed by Chouet (1992), the different energy of the initial high-frequency wave trains of the signals is explained by differences in the source time function of the pressure pulse that triggers the oscillation of the fluid-filled crack. When the rise time is sharp, we observe the highest energy of the high-frequency waves. A smooth source time function will reduce the high-frequency contribution to the spectrum. When the pressure step appears isolated, the duration of the resulting signal is short and produces an LP event. In the case of continuous or multiple activation of the source, the resulting signal may last for minutes or hours, producing volcanic tremor. Note that some of the seismo-volcanic events recorded at Deception Island during the 1994–1997 period were classified as hybrids (Ibáñez et al., 2000) based on their spectral properties; however, they may not represent true hybrids as described for example by Lahr et al. (1994) for Redoubt volcano. They can be explained by the same source mechanism described above, and therefore may be better considered as LP events with an energetic high-frequency onset. Finally, we must point out that the conceptual model of single crack in Fig. 10 is an over-simplification. In reality, the source may be composed of a complex crack system with different sizes and orientations.

Due to its characteristic spectral properties, the quasi-monochromatic tremor may be explained by a different mechanism, consisting of the resonance of a pipe-like conduit (Chouet, 1985). The signals show spectral peaks that are overtones of a fundamental frequency. This spectral pattern reveals that one dimension of the source is dominant over the other two, and therefore an organ pipe source model would be adequate to explain the spectral features of the tremor.

5.2. *VT earthquake source model*

To understand a fracture process involving low stress drop, small fault dimensions, and occurrence of multiplets, as observed in Deception Island, Ibáñez et al. (2003) invoked the role of the fluids. In this framework the release of seismic energy is associated with lubrication of a pre-existing zone of weakness. Lubrication reduces the friction coefficient and decreases the effective normal stress over the fault surface. This can in turn trigger the

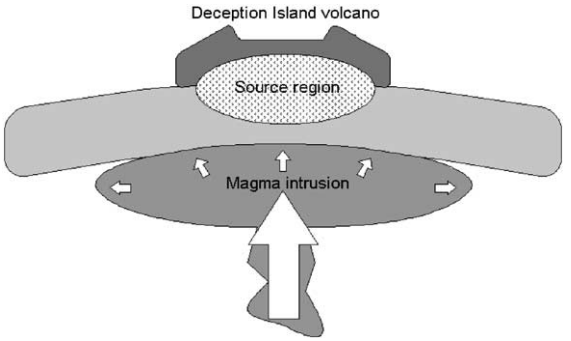

Fig. 11. Sketch of the deep magma intrusion model proposed by Ibáñez et al. (2003) for the origin of the 1999 VT series at Deception Island volcano (see text for explanations).

earthquake. Ibáñez et al. (2003) proposed a possible scenario that explained the origin of the seismic crisis based on the volcanic nature of Deception Island. The seismic series was caused by stress generated by the uplift of the source area in response to the injection of magma at depth (Fig. 11). The presence of a magma reservoir in the northeast area of Port Foster has been suggested by several authors (Blanco, 1997; García et al., 1997). An increase of pressure within the magma reservoir, or the upward displacement of magma, disturbs the stress field in the region over the reservoir. When the stress reaches a threshold value, fracture processes begin, following pre-existing zones of weakness. The absence of visible evidence of a subsequent eruption and the lower level of earthquake activity observed since 1999 imply that the injection of magma stopped before reaching of the surface. The uplift hypothesis is compatible with the majority of the geophysical observations. The small size of the fractures involved is explained by lubrication of the microfaults due to pressurized fluids. The increase of pore pressure in the very shallow crust overlying the magmatic system could have induced the repeated activation of the fracture network. The presence of fluids in the source area not only expedites the fracture processes, but also explains the origin of the hybrids. Their low-frequency segments are produced by resonances of fluid-filled cracks. The fluid involved in the lubrication of the microfaults and the generation of hybrid events is probably not magmatic, but water embedded in the geological structure. Martini and Giannini (1988) reported the existence of a shallow aquifer near the epicentral area, and a deeper aquifer may be present as well (Martini and Casselli, pers. comm.).

6. Conclusions

The data obtained since 1986 during several seismic field surveys at Deception Island demonstrate that this is a seismically active volcano. Both LP seismicity and VT earthquakes have been recorded and analyzed, leading to knowledge of different aspects of the volcano. The present paper describes this seismicity and proposes models that may realistically explain the release of seismic energy within the volcano.

The most intense seismic activity at Deception Island occurred during the seismic crises of 1992 and 1999. This means that in about 15 years of seismic monitoring, two intense volcanic crises have been observed. If we take into account that there are no permanent stations on the island, and seismic measurements can be performed only during 3 months/yr (from December to February), then similar periods of intense seismic activity might be occurring more often than what has been detected so far. Deception Island, therefore, seems to be a very active volcano, at least from a seismological point of view, although no eruption has been reported since 1970. Given the frequent presence of scientific teams, and also thousands of tourists (especially during the summer season), greater efforts should be put into seismic and geophysical monitoring of Deception Island in order to reduce the risk associated with volcanic hazards.

Acknowledgements

This work was partially supported by projects ANT98-1111, REN-2000-2897, EU project e-Ruption EVR1-2001-00024, and REN-2001-3833. We thank five anonymous reviewers and the

editors of this special volume. Their reviews helped to improve significantly this manuscript.

References

Alguacil, G., Almendros, J., Del Pezzo, E., García, A., Ibáñez, J.M., La Rocca, M., Morales, J., Ortiz, R., 1999. Observations of volcanic earthquakes and tremor at Deception Island, Antarctica. Annali di Geofisica 42, 417–436.

Almendros, J., Ibáñez, J.M., Alguacil, G., Del Pezzo, E., Ortiz, R., 1997. Array tracking of the volcanic tremor source at Deception Island, Antarctica. Geophysical Research Letters 24, 3069–3072.

Almendros, J., Ibáñez, J.M., Alguacil, G., Del Pezzo, E., 1999. Array analysis using circular wave-front geometry: an application to locate the nearby seismo-volcanic source. Geophysical Journal International 136, 159–170.

Almendros, J., Chouet, B., Dawson, P., 2001. Spatial extent of a hydrothermal system at Kilauea volcano, Hawaii, determined from array analyses of shallow long-period seismicity, 2. Results. Journal of Geophysical Research 106, 12318–12330.

Aristarain, A.J., Delmas, R.J., 1998. Ice record of a large eruption of Deception Island volcano (Antarctica) in the XVIIth century. Journal of Volcanology and Geothermal Research 80, 17–25.

Bacon, C.R., 1985. Implications of silicic vent patterns for the presence of large crustal magma chambers. Journal of Geophysical Research 90, 11243–11252.

Baker, P.E., Davis, T.G., Roobol, M.J., 1969. Volcanic activity at Deception Island in 1967 and 1969. Nature 224, 553–560.

Baker, P.E., McReath, I., Harvey, M.R., Roobol, M.J., Davis, T.G., 1975. The Geology of the South Shetland Islands: V. Volcanic evolution of Deception Island. British Antarctic Survey Scientific Reports 78, 81pp.

Barker, P.F., 1982. The Cenozoic subduction history of the Pacific margin of the Antarctic Peninsula: ridge crest-trench interactions. Journal of the Geological Society of London 139, 787–801.

Barker, D.H., Austin, J.A., 1994. Crustal diapirism in Bransfield Strait, West Antarctica: evidence for distributed extension in marginal-basin formation. Geology 22, 657–660.

Barker, D.H., Austin, J.A., 1998. Rift propagation, detachment faulting, and associated magmatism in Bransfield Strait, Antarctic Peninsula. Journal of Geophysical Research 103, 24017–24043.

Barker, D.H., Christeson, G.L., Austin, J.A., 2001. Crustal structure of an active backarc basin at the rift-drift transition: Bransfield Strait, Antarctica. EOS Transaction of the AGU Fall Meeting Supplement 82(47), pp. F1244 (abstract).

Bialas, J., Meissner, R., Miller, H., Fluh, E., Parker, T., Henriet, J.P., Hedrich, K., Heuverswyn, E.V., Jokat, W., Wever, T., 1990. Preliminary results of seismic reflection investigations and associated geophysical studies in the area of the Antarctic Peninsula. Antarctic Science 2, 223–234.

Birkemajer, K., 1992. Volcanic succession at Deception Island, West Antarctica: a revised lithostratigraphic standard. Studia Geological Polonica 101, 27–82.

Blanco, I., 1997. Análisis e interpretación de las anomalías magnéticas de tres calderas volcánicas: Decepción (Shetland del Sur, Antátida), Furnas (San Miguel, Azores) y las Cañadas del Teide (Tenerife, Canarias). Ph.D. Thesis, Universidad Complutense de Madrid, 250pp.

Brune, J.N., 1970. Tectonic stress and the spectra of seismic shear waves. Journal of Geophysical Research 89, 1132–1146.

Chouet, B., 1985. Excitation of a buried magmatic pipe: a seismic source model for volcanic tremor. Journal of Geophysical Research 90, 1881–1893.

Chouet, B., 1986. Dynamics of a fluid-driven crack in three dimensions by the finite difference method. Journal of Geophysical Research 91, 13967–13992.

Chouet, B., 1988. Resonance of a fluid-driven crack: radiation properties and implications for the source of long-period events and harmonic tremor. Journal of Geophysical Research 93, 4375–4400.

Chouet, B., 1992. A seismic model for the source of long-period events and harmonic tremor. In: Aki, K., Gasparini, P., Scarpa, R. (Eds.), Volcanic Seismology (IAVCEI Proceedings in Volcanology 3). Springer, Berlin, pp. 133–156.

Chouet, B., 1996. Long-period volcano seismicity: its source and use in eruption forecasting. Nature 380, 309–316.

Cooper, A.P.R., Smellie, J.L., Maylin, J., 1998. Evidence for shallowing and uplift from bathymetric records of Deception Island, Antarctica. Antarctic Science 10, 455–461.

Correig, A.M., Urquizu, M., Vila, J., Martí, J., 1997. Analysis of the occurrence of seismicity at Deception Island (Antarctica): a nonlinear approach. Pure and Applied Geophysics 149, 553–574.

Dietrich, R., Dach, R., Engelhardt, G., Ihde, J., Korth, W., Kutterer, H.J., others, 2001. ITRF coordinates and plate velocities from repeated GPS campaigns in Antarctica—an analysis based on different individual solutions. Journal of Geodesy 74, 756–766.

Felpeto, A., Blanco, I., Del Rey, R., Morales, J., 1994. Estudios de eventos de baja frecuencia registrados en Isla Decepción (in Spanish). In: Cacho, J., Serrat, D. (Eds.), Actas del V Simposio de Estudios Antárticos, CICYT, Barcelona pp. 147–154.

García, A., Blanco, I., Torta, J.M., Astiz, M., Ibáñez, J.M., Ortiz, R., 1997. A search for the volcanomagnetic signal at Deception volcano (South Shetland Islands, Antarctica). Annali di Geofisica 40, 319–327.

Gracia, E., Canals, M., Farran, M.L., Prieto, M.J., Sorribas, J., 1996. Morphostructure and evolution of the Central and Eastern Bransfield basins (NW Antarctic Peninsula). Marine Geophysical Researches 18, 429–448.

Gracia, E., Canals, M., Farran, M.L., Sorribas, J., Pallas, R., 1997. Central and Eastern Bransfield basins (Antarctica)

from high-resolution swath-bathymetry data. Antarctic Science 9, 168–180.

Grad, M., Guterch, A., Sroda, P., 1992. Upper crustal structure of Deception Island area, Bransfield Strait, West Antarctica. Antarctic Science 4, 469–476.

Grad, M., Shiobara, H., Janik, T., Guterch, A., Shimamura, H., 1997. Crustal model of Bransfield Rift, West Antarctica, from detailed OBS refraction experiments. Geophysical Journal International 130, 506–518.

Havskov, J., Peña, J.A., Ibáñez, J.M., Ottemöller, L., Martinez-Arévalo, C., 2003. Magnitude scales for very local earthquakes: application to Deception Island volcano (Antarctica). Journal of Volcanology and Geothermal Research, in press.

Ibáñez, J.M., Morales, J., Alguacil, G., Almendros, J., Ortiz, R., Del Pezzo, E., 1997. Intermediate focus earthquakes under South Shetland Islands (Antarctica). Geophysical Research Letters 24, 531–534.

Ibáñez, J.M., Del Pezzo, E., Almendros, J., La Rocca, M., Alguacil, G., Ortiz, R., García, A., 2000. Seismovolcanic signals at Deception Island volcano, Antarctica: wave field analysis and source modeling. Journal of Geophysical Research 105, 13905–13931.

Ibáñez, J.M., Carmona, E., Almendros, J., Saccorotti, G., Del Pezzo, E., Abril, M., Ortiz, R., 2003. The 1998–1999 seismic series at Deception Island volcano, Antarctica. Journal of Volcanology and Geothermal Research, in press.

Janik, T., 1997. Seismic crustal structure of the Bransfield Strait, West Antarctica. Polish Polar Research 18, 171–225.

Julian, B.R., 1994. Volcanic tremor: nonlinear excitation by fluid flow. Journal of Geophysical Research 99, 11859–11877.

Keller, R.A., Fisk, M.R., White, W.M., 1991. Geochemistry of quaternary volcanism in the Bransfield Strait and South Shetland Islands: preliminary results. Antarctic Journal of the United States 26, 132–133.

Kim, Y., Kim, H.-S., Larter, R.D., Camerlenghi, A., Gamboa, L.A., Rudowski, S., 1995. Tectonic deformation in the upper crust and sediments at the South Shetland Trench. In: Cooper, A.K., Barker, P.F., Brancolini, G. (Eds.), Geology and Seismic Stratigraphy of the Antarctic Margin. Antarctic Research Series 68, American Geophysical Union, Washington, DC, pp. 157–166.

Lahr, J., Chouet, B., Stephens, C., Power, J., Page, R., 1994. Earthquake classification, location and error analysis in a volcanic environment: implications for the magmatic system of the 1989–1990 eruptions at Redoubt volcano, Alaska. Journal of Volcanology and Geothermal Research 62, 137–151.

Lawver, L.A., Keller, R.A., Fisk, M.R., Strelin, J.A., 1995. Bransfield Strait, Antarctic Peninsula: active extension behind a dead arc. In: Taylor, B. (Ed.), Backarc Basins: Tectonics and Magmatism. Plenum Press, New York, pp. 315–342.

Lawver, L.A., Sloan, B.J., Barker, D.H., Ghidella, M., Von Herzen, R.P., Keller, R.A., Klinkhammer, G.P., Chin, C.S., 1996. Distributed, active extension in Bransfield Basin, Antarctic Peninsula: evidence from multibeam bathymetry. GSA Today 13, 2–6.

Lee, D.K., Kim, Y.D., Nam, S.H., Jin, Y.K., 1998. Local seismic activity monitored at King Sejong Station, Antarctica. Polar Geoscience 11, 76–89.

Madariaga, R., 1977. High-frequency radiation from crack (stress drop) models of earthquakes faulting. Geophysical Journal of Royal Astronomical Society 51, 625–652.

Martí, J., Baraldo, A., 1990. Pre-caldera pyroclastic deposits of Deception Island (South Shetland Islands). Antarctic Science 2, 345–352.

Martí, J., Vila, J., Rey, J., 1996. Deception Island (Bransfield Strait, Antarctica): an example of volcanic caldera developed by extensional tectonics. In: McGuire, W., Jones, A., Neuberg, J. (Eds.), Volcano Instability on the Earth and other Planets, Vol. 110. Geological Society Special Publication 110, London, pp. 253–265.

Martínez-Arévalo, C., Bianco, F., Ibáñez, J.M., Del Pezzo, E., 2003. Shallow seismic attenuation in the short period range of Deception Island volcano (Antarctica). Journal of Volcanology and Geothermal Research, in press.

Martini, M., Giannini, L., 1988. Deception Island (South Shetlands): an area of active volcanism in Antarctica. Memorie della Societa Geologica Italiana 43, 117–122.

Newhall, C.G., Dzurisin, D., 1988. Deception Island. In: Historical unrest at large calderas of the world. US Geological Survey Bulletin 1855, pp. 1013–1019.

Orheim, O., 1972. Volcanic activity on Deception Island, South Shetland Islands. In: Adie, R.J. (Ed.), Antarctic Geology and Geophysics. Universitetsforlaget, Oslo, pp. 117–120.

Ortiz, R., Vila, J., García, A., Camacho, A.G., Díez, J.L., Aparicio, A., Soto, R., Viramonte, J.G., Risso, C., Menegatti, N., Petrinovic, I., 1992. Geophysical features of Deception Island. In: Yoshida, Y., Kaminamura, K., Shiraishi, K. (Eds.), Recent Progress in Antarctic Earth Science. Terrapub, Tokyo, pp. 443–448.

Ortiz, R., García, A., Aparicio, A., Blanco, I., Felpeto, A., Del Rey, R., Villegas, M., Ibáñez, J.M., Morales, J., Del Pezzo, E., Olmedillas, J.C., Astiz, M., Vila, J., Ramos, M., Viramonte, J.G., Risso, C., Caselli, A., 1997. Monitoring of the volcanic activity of Deception Island, South Shetland Islands, Antarctica (1986–1995). In: Ricci, C.A. (Ed.) The Antarctic Region: Geological Evolution and Processes, Terra Antartica Publication, Siena, pp. 1071–1076.

Pelayo, A.M., Wiens, D.A., 1989. Seismotectonics and relative plate motions in the Scotia Sea region. Journal of Geophysical Research 94, 7293–7320.

Prieto, M.J., Canals, M., Ercilla, G., de Batist, M., 1998. Structure and geodynamic evolution of the Central Bransfield Basin (NW Antarctica) from seismic reflection data. Marine Geology 149, 17–38.

Rey, J., Somoza, L., Martínez-Frías, J., 1995. Tectonic, volcanic, and hydrothermal event sequence on Deception Island (Antarctica). Geo-Marine Letters 15, 1–8.

Rey, J., Somoza, L., Martínez-Frías, J., Benito, R., Martín-Alfageme, S., 1997. Deception Island (Antarctica): a new target for exploration of Fe–Mn mineralization? In:

Nicholson, K., Hein, J.R., Buhn, B., Dasgupta, S. (Eds.), Manganese Mineralization: Geochemistry and Mineralogy of Terrestrial and Marine Deposits, Geological Society Special Publication 119, London, pp. 239–251.

Robertson, S.D., Wiens, D.A., Dorman, L.M., Shore, P.J., Vera, E., 2001. Seismicity and tectonics of the South Shetland Islands region from a combined land-sea seismograph deployment. EOS Transaction of the AGU Fall Meeting Supplement 82(47), pp. F818 (abstract).

Roobol, M.J., 1973. Historic volcanic activity at Deception Island. British Antarctic Survey Bulletin 32, 23–30.

Roobol, M.J., 1979. A model for the eruptive mechanism of Deception Island from 1820 to 1970. British Antarctic Survey Bulletin 49, 137–156.

Roobol, M.J., 1982. The volcanic hazard at Deception Island, South Shetland Islands. British Antarctic Survey Bulletin 51, 237–245.

Smellie, J.L., 1988. Recent observations on the volcanic history of Deception Island, South Shetland Islands. British Antarctic Survey Bulletin 81, 83–85.

Smellie, J.L., 1990. Deception Island. In: LeMasurier, W.E., Thomson, J.W. (Eds.), Volcanoes of the Antarctic Plate and Southern Oceans. American Geophysical Union, Washington, DC, pp. 316–321.

Vila, J., Martí, J., Ortiz, R., García, A., Correig, A.M., 1992. Volcanic tremors at Deception Island (South Shetland Islands, Antarctica). Journal of Volcanology and Geothermal Research 53, 89–102.

Vila, J., Correig, A.M., Martí, J., 1995. Attenuation and source parameters at Deception Island (South Shetland Islands, Antarctica). Pure and Applied Geophysics 144, 229–250.

Walker, G.P., 1984. Downsag calderas, ring faults, caldera sizes, and incremental caldera growth. Journal of Geophysical Research 89, 8407–8416.